



AD-A209 030

REPORT DOCUMENTATION PAGE

2b. DECLASSIFICATION / DOWNGRADING SCHEDULE		1b. RESTRICTIVE MARKINGS	
4. PERFORMING ORGANIZATION REPORT NUMBER(S)		3. DISTRIBUTION / AVAILABILITY OF REPORT Approved for public release; distribution unlimited.	
6a. NAME OF PERFORMING ORGANIZATION Scientific Research Associates, Inc.		5. MONITORING ORGANIZATION REPORT NUMBER(S) ARO 26239.1-EG-SBI	
6b. OFFICE SYMBOL (if applicable)		7a. NAME OF MONITORING ORGANIZATION U. S. Army Research Office	
6c. ADDRESS (City, State, and ZIP Code) 50 Nye Road Glastonbury, Connecticut 06033		7b. ADDRESS (City, State, and ZIP Code) P. O. Box 12211 Research Triangle Park, NC 27709-2211	
8a. NAME OF FUNDING / SPONSORING ORGANIZATION U. S. Army Research Office		9. PROCUREMENT INSTRUMENT IDENTIFICATION NUMBER DAAL03-88-C-0028	
8b. OFFICE SYMBOL (if applicable)		10. SOURCE OF FUNDING NUMBERS	
8c. ADDRESS (City, State, and ZIP Code) P. O. Box 12211 Research Triangle Park, NC 27709-2211		PROGRAM ELEMENT NO.	PROJECT NO.
		TASK NO.	WORK UNIT ACCESSION NO.
11. TITLE (Include Security Classification) Hypersonic Vehicle Environment Simulation			
12. PERSONAL AUTHOR(S) F. I. de Jong, I. S. Sabnis, and H. McDonald			
13a. TYPE OF REPORT Final		14. DATE OF REPORT (Year, Month, Day) May 1989	
13b. TIME COVERED FROM 8/1/88 TO 3/31/89		15. PAGE COUNT 36	
16. SUPPLEMENTARY NOTATION The view, opinions and/or findings contained in this report are those of the author(s) and should not be construed as an official Department of the Army position, policy, or decision, unless so designated by other documentation.			
17. COSATI CODES		18. SUBJECT TERMS (Continue on reverse if necessary and identify by block number)	
FIELD	GROUP	Fluid Dynamics, Flow Fields, Hypersonic Vehicle Environment Simulation, Vehicle Performance, Hypersonic Flow, Chemical Reactions	
19. ABSTRACT (Continue on reverse if necessary and identify by block number)			
<p>The hypersonic, viscous, chemically reacting flow around a vehicle in the upper layers of the atmosphere influences vehicle performance, thermal environment, and sensor visibility. Under the Phase I effort, a unique hybrid Navier-Stokes/Monte Carlo method has been successfully developed for the simulation of said hypersonic flows. This method combines a continuum description of the gas mixture with a statistical (or "particle") description of the species</p>			
20. DISTRIBUTION / AVAILABILITY OF ABSTRACT <input type="checkbox"/> UNCLASSIFIED/UNLIMITED <input type="checkbox"/> SAME AS RPT. <input type="checkbox"/> DTIC USERS		21. ABSTRACT SECURITY CLASSIFICATION Unclassified	
22a. NAME OF RESPONSIBLE INDIVIDUAL		22b. TELEPHONE (Include Area Code)	22c. OFFICE SYMBOL

DTIC ELECTED JUN 6 1989

transport and the chemical reactions, thereby allowing easy use of available chemical kinetics data. As such, the hybrid approach is capable of exploiting both the efficiency of a continuum approach for the fluid dynamic calculations and the benefits in physical modeling of the Monte Carlo approach for chemical reactions. The viability of this hybrid approach for practical hypersonic flow calculations has been demonstrated in the Phase I effort via the calculation of the chemically reacting flow field over an axisymmetric cone.

# Scientific Research Associates, inc.

50 Nye Road, P.O. Box 1058  
 Glastonbury, Connecticut 06033  
 (203) 659-0333 FAX (203) 633-0676

HYPERSONIC VEHICLE ENVIRONMENT SIMULATION

F.J. de Jong, J.S. Sabnis, and H. McDonald

FINAL REPORT - SBIR PHASE I

Contract DAAL03-88-C-0028

Prepared for:

U.S. Army Research Office  
 Research Triangle Park, NC

<b>Accession For</b>	
NTIS GRA&I	<input checked="" type="checkbox"/>
DTIC TAB	<input type="checkbox"/>
Unannounced	<input type="checkbox"/>
Justification	
By _____	
Distribution/	
<b>Availability Codes</b>	
<b>Dist</b>	<b>Avail and/or Special</b>
A-1	



May 1989

# HYPERSONIC VEHICLE ENVIRONMENT SIMULATION

## PHASE I - FINAL REPORT

F. J. de Jong, J.S. Sabnis, and H. McDonald  
Scientific Research Associates, Inc.  
Glastonbury, Connecticut

### PROJECT SUMMARY

The hypersonic, viscous, chemically reacting flow around a vehicle in the upper layers of the atmosphere influences vehicle performance, thermal environment, and sensor visibility. Under the Phase I effort, a unique hybrid Navier-Stokes/Monte Carlo method has been successfully developed for the simulation of said hypersonic flows. This method combines a continuum description of the gas mixture with a statistical (or "particle") description of the species transport and the chemical reactions, thereby allowing easy use of available chemical kinetics data. As such, the hybrid approach is capable of exploiting both the efficiency of a continuum approach for the fluid dynamic calculations and the benefits in physical modeling of the Monte Carlo approach for chemical reactions. The viability of this hybrid approach for practical hypersonic flow calculations has been demonstrated in the Phase I effort via the calculation of the chemically reacting flow field over an axisymmetric cone. A proposed Phase II effort would continue the development of this method by improving the numerical efficiency of the particle transport scheme, and by incorporating physical models for catalytic walls, recombination reactions, and ionization. In addition, radiation would be included via a radiation transport model. For the class of problems of interest here, the resulting procedure will be able to represent the complex chemical and thermal processes occurring around a hypersonic vehicle in much more detail than is currently possible with either the continuum or the direct simulation Monte Carlo (DSMC) approach. The proposed Phase II program would also modify the computer code for use in a workstation environment via the development of suitable input and output packages, thus producing a valuable design tool for the examination of the thermal environment and the sensor visibility of hypersonic vehicles.

## Table of Contents

1. Introduction . . . . .	.1
2. Background . . . . .	2
3. The Hybrid Navier-Stokes/Monte Carlo Method. . . . .	6
3.1 Step 1. - The Continuum Phase . . . . .	7
3.2 Step 2. - The Species Transport Phase . . . . .	.10
3.3 Step 3. - The Chemical Reaction phase . . . . .	.13
3.4 Coupling of the Three Phases. . . . .	.17
4. Results and Conclusions. . . . .	.18
5. Future Development . . . . .	.32
References . . . . .	.34

## 1. INTRODUCTION

Ground or air launched interceptors can achieve high velocities ( $> 3$  kft/sec) within the atmosphere either during the boost or intercept phase of their mission. Space launched interceptors may also find it advantageous to be able to penetrate the atmosphere to enlarge their domain of effectiveness. The high velocities necessary to achieve successful interception result in high Mach numbers ( $> 10$ ) within the atmosphere ( $< 300$  kft). The resulting frictional heating of the boundary layer and the collisional heating due to the bow shock create gas temperatures that are sufficiently high ( $> 6000$  K) that significant energy is absorbed in disassociating the air and significant energy transport can occur by radiation. This radiation is complicated by the fact that the gas is partly disassociated. The disassociation and radiation causes two specific concerns. The first is the subsequent additional thermal loading over and above the normal convective load on the thermal protection system due to recombination and radiative transfer effects which, if known, could be accounted for in the design. The second concern is potentially more important since it bears on the vehicle functionality and relates to the vehicle signature and the ability of sensors to see source radiant energy through this complex, vehicle-induced chemical and radiative environment.

Insofar as this source radiant energy is concerned, it is not simply the integrated flux at the sensor that is required, but the distribution across the spectrum is of interest, for purposes of sensor design and source identification. The transmission of this source radiant energy through the vehicle environment unfortunately depends on the gas composition and temperature, since the absorption and emissivity are functions of both. As a result, certain frequencies suffer much more absorption than others, particularly at the lower temperatures and at frequencies around  $4000\text{\AA}$  ( $.4\mu\text{m}$ ), the near infrared, but the extent is a very complex issue requiring very detailed information on the local gas composition and temperature.

Potential additional complication in an already complex problem arises with active cooling of the vehicle boundary layer or ablation. Such coolant would reduce or change the radiation from the boundary layer, but also would absorb radiation from the shock. Note also that the boundary layer, the coolant flow and the shock structure are very strongly interacting in hypersonic flow and thus a coupled flow, chemistry analysis and radiation would seem appropriate. The degree

to which the vehicle thermal environment as well as radiation at the sensor would change due to coolant flow is difficult to estimate without doing a very precise computation.

It is further observed that the shock wave structure, particularly the bow structure, is very important in setting the flow and thermal fields (via the temperature), the radiation field and the degree of disassociation (which also influences the temperature), which in turn greatly influences the spectral distribution of radiation emissivity and absorptivity. This shock structure, location, and strength in terms of pressure and temperature rise is in turn determined by the forebody geometry, incidence, flight velocity and altitude. Thus, forebody geometry at a particular flight condition could be examined and varied to see if a beneficial impact on signature, thermal environment and sensor visibility could be achieved. However, in order to make such an assessment, very detailed, coupled reacting flow and radiation field predictions are necessary. It is the development of a procedure for efficiently making these calculations and the performance of these predictions that is the subject of the present Phase I and the proposed Phase II effort. Some of the complexities of the flow field around this type of vehicle are illustrated in the volume edited by Nelson (Ref. 1).

## 2. BACKGROUND

The major task that has to be performed is the development of a hybrid viscous flow field Computational Fluid Dynamics (CFD) prediction code which would be suitable for efficiently determining the vehicle flow and thermal environment, including the effects of disassociation and radiation, at high Mach numbers within the atmosphere. During the Phase I effort the major emphasis has been placed upon demonstrating the potential of a unique hybrid Navier-Stokes/Monte Carlo method with particular emphasis upon disassociation. The proposed Phase II effort would continue the Phase I disassociation work and also incorporate a radiation capability within this unique procedure. Before proceeding, it is useful to consider possible approaches to solving the high altitude, high Mach number external flow problem. These approaches include usual Navier-Stokes procedures, usual Monte-Carlo procedures and the unique procedure demonstrated in the Phase I effort. The following discussion indicates the advantages of the Phase I approach for the class of problems of interest here.

In regard to candidate codes, most existing three-dimensional Navier-Stokes codes could be modified to include radiative transport by adding the appropriate term in the energy equation and incorporating a radiative transport equation. The choice of the most suitable Navier-Stokes code is not primarily determined by radiative effects. The situation in regard to chemical reaction is different. In recent years, there has been a considerable increase in the number of potentially applicable reacting flow codes, such as the axisymmetric codes of Candler and McCormack (Ref. 2) and Green (Ref. 3), for instance. While codes such as those of Refs. 2 and 3 are based on the continuum flow equations, even conceptually more general codes based on the direct simulation of molecular dynamics using the kinetic theory of gases have been constructed, for instance by Moss and Bird (Ref. 4). While such direct simulation codes are of great theoretical interest, they are currently not practical in terms of flow dimensionality and computer run time for the near continuum and continuum flow regime and will require much development before they can address the present problem in any detail. Appropriate codes based on the continuum equations are much further along in the development, although, for instance, the codes of Refs. 2 and 3 are currently restricted to axisymmetric flow, but this restriction could be easily removed.

At the proposed flight conditions the flow field becomes disassociated behind the bow shock and the temperature field reflects the energy required to disassociate, and in some instances ionize, the air. In the subsequent recombination of the species some of this energy is given up, thus the time scale of the relaxation can have a major influence on the thermal protection system, since the relaxation process governs the degree and location of the heat release. The molecules are also vibrationally and rotationally excited and this can also serve to store energy. Thus a realistic simulation of the flow field requires a large number of distinct species be tracked. Depending on the quantities of interest, chemists have determined that as few as five species or as many as thirty or more may be required (Refs. 4, 5). To this is added one grouping for each of the excited states that are required, including the ionized species. In the conventional continuum approach, as exemplified by schemes such as those in Refs. 2 and 3, the resulting set requires one partial differential equation for each species or state (Ref. 6). Very quickly the labor of solving the chemistry greatly exceeds that of solving the fluid conservation equations. For instance, in two dimensions, in the typical block implicit approach, such as in Ref. 2, five

species and three vibrationally excited molecules are followed, resulting in an  $(11/4)^3$ -fold increase in run time relative to solving for a perfect gas, i.e.,

$$F = \frac{\text{run time, reacting}}{\text{run time, perfect gas}} = \left[ \frac{N_s - 1 + N_f}{N_f} \right]^3$$

where  $N_f$  is the number of equations in the fluids system (four in two dimensions, five in three dimensions),  $N_s$  is the number of distinct species or states, and  $F$  represents the ratio of run times (note - Ref. 2 gives  $F$  as proportional to the square of the number of species, however, standard textbooks give the operation count of a block tridiagonal system as going as the cube of the block size).

There are various strategies for reducing the run time of these implicit approaches, attempting to make it more nearly proportional to the ratio  $(N_s - 1 + N_f)/N_f$ , rather than the cube of this ratio. Depending on the specific reactions involved, these strategies may or may not be successful, conditional on the stiffness of the system and its size. Nonetheless, at present no clearly superior general uncoupled alternative has yet appeared.

In free molecular and near free molecular flow it is computationally feasible to follow individual molecules and determine the appropriate fluxes by averaging over many trials. Such molecule-by-molecule simulation using the kinetic theory of gases contains a random selection process which has become associated with the name 'Monte Carlo' methodologies. Within the Monte Carlo framework there are a multitude of different equations and methods. In gas dynamics a particular variant has been termed the Direct Simulation Monte Carlo (DSMC) method. The DSMC method is described in detail in the book by Bird (Ref. 7), and involves following groups of molecules rather than individual molecules. The various groups are interacted in a probabilistic manner. Thus the approach may be thought of as representing the gas by a smaller than actual number of real molecules or alternatively as a model gas with the actual number of larger model gas molecules. Bird (Refs. 7, 8) has shown how DSMC can be extended to chemically reacting flow using the principles of the kinetic theory of gases in a very straightforward manner. Here the computational run time goes only (linearly) as the increased number of molecules required to statistically describe the extended system. Bird also points out that the overall scheme becomes computationally more and more expensive as the Knudsen number becomes smaller, such that below  $Kn \approx .1$  the method is probably unworkable in two or three space dimensions. Here the problem is the requirement that the typical cell size be much smaller than the mean free path.

Thus there is a dilemma. The well understood implicit continuum methods for reacting flow have a computational effort that increases as the cube of the number of species, but to obtain reasonable computer run times from DSMC, where the run time goes linearly with the number of molecules, one requires a very dilute gas with a cell size small compared to the mean free path. The present effort suggests an innovative alternative hybrid 'two-phase flow' approach. The mean motion of the gas is described in an Eulerian frame, the 'continuum gas phase' of the 'two phase flow'. The simulated molecular phase is described in a Lagrangian frame, the 'solid particle' phase of the two phase flow. In the usual two phase flow manner the particles are convected by the mean flow. However, the particles are now interpreted in the manner of Direct Simulation Monte Carlo as groups of molecules. The various groups are interacted in the same probabilistic manner used in the DSMC method, including the chemical interactions. The mixture continuum gas phase is then recomputed using the species concentrations resulting from the particulate phase. Either at each time step of a transient problem or upon reaching steady state as the asymptote of an unsteady problem, the gas and particulate phases would be iterated until both 'phases' were in computational equilibrium. Chemical and thermodynamic equilibrium would not be a requirement, however, other than in the implied Maxwellian form for the random molecular velocity in the continuum equations.

Intuitively, a large enough chemical system could always be chosen such that the hybrid approach would eventually be more economical than solving a large system of coupled partial differential equations. However, within the continuum approach strategies do exist for treating the coupled chemical-fluid system in an uncoupled manner. From a computational chemistry viewpoint, a completely uncoupled explicit treatment of the chemical system is not general and usually is very inefficient with the normal stiff chemical systems. Indeed, the chemistry problem created the impetus for the whole field of stiff ordinary differential equation system solvers. Depending on how uncoupled the system is physically and to what extent it has been assumed uncoupled computationally, the degree of iteration necessary to reintroduce the system coupling into the uncoupled computation may be very significant. The current view is that sufficient physical coupling exists for the case where the air chemistry around the vehicle is of interest, to require the coupled system approach which, as previously noted, at best has a labor that goes as the cube of the system size. The hybrid approach outlined here does introduce similar coupling concerns, since the chemistry and

fluid are essentially uncoupled over each time step or pseudo time step/iteration. Thus, it is highly desirable to reduce the labor of both the direct molecular simulation step and the fluids step as much as possible, so that the labor of iteratively coupling the two systems will not be great. Much effort by a large number of people is currently underway to reduce the required fluids computational effort for a multitude of other reasons, and Scientific Research Associates, Inc. is actively following the literature and participating in these developments. As a result, it is only necessary here to consider the efficiency of the Monte Carlo part of the calculation.

The hybrid approach developed in the Phase I investigation is capable of exploiting both the efficiency of a continuum approach for the fluid dynamic calculation of the gas mixture and the benefits in physical modeling of the Monte Carlo approach for the chemical reactions. For the class of problems of interest here, this approach will be able to represent the complex chemical and thermal processes more efficiently than a DSMC approach and more accurately than a conventional Navier-Stokes procedure.

### 3. THE HYBRID NAVIER-STOKES/MONTE CARLO METHOD

The hybrid method developed under the present effort allows the analysis of chemically reacting gas flows around a vehicle traveling at hypersonic speeds within the atmosphere. In this method, the Navier-Stokes equations are used to model the gas flow, while a Monte Carlo-like technique is used to simulate the chemical reactions. For each small time interval  $\Delta t_m$ , the following steps are taken:

- (1) The Navier-Stokes equations are solved numerically for the mean flow field, together with the global continuity and energy equations for the gas mixture, assuming "frozen" species concentrations.
- (2) Computational particles representing the species molecules are transported, using convection velocities computed in (1) and taking into account molecular diffusion of the species.

(3) A representative set of reactions is computed among the particles by means of DSMC-like techniques. The post-reaction particle distribution is used to update the species concentrations.

A detailed description of each of the steps of the hybrid Navier-Stokes/Monte Carlo method is presented below.

### 3.1. Step 1. - The Continuum Phase

In the continuum phase, the mean flow field calculations are performed via numerical solution of the Navier-Stokes equations, and the global continuity and energy equations for the gas mixture. In vector form this set of equations can be written as

$$\frac{\partial \rho}{\partial t} + \nabla \cdot \rho \mathbf{U} = 0 \quad (1)$$

$$\frac{\partial (\rho \mathbf{U})}{\partial t} + \nabla \cdot (\rho \mathbf{U} \mathbf{U}) = -\nabla p + \nabla \cdot \tau \quad (2)$$

$$\frac{\partial (\rho h)}{\partial t} + \nabla \cdot (\rho \mathbf{U} h) = \frac{Dp}{Dt} + \Phi - \nabla \cdot \mathbf{q} + r \quad (3)$$

where  $\rho$  is the density of the mixture,  $\mathbf{U}$  is the velocity,  $p$  is the pressure,  $\tau$  is the stress tensor (molecular and turbulent),  $h$  is the mixture enthalpy (including the heat of formation),  $\Phi$  is the viscous dissipation per unit volume,  $\mathbf{q}$  is the heat flux vector, and  $r$  is the radiation term.  $D/Dt$  denotes a material derivative, i.e.  $D/Dt = \partial/\partial t + \mathbf{U} \cdot \nabla$ .

It should be noted that the use of the Navier-Stokes equations with its usual stress strain relationship is consistent with a Maxwellian distribution of the molecular random velocities (see Ref. 7).

The above equations for the gas mixture have to be supplemented by the equation of state for an ideal gas mixture,

$$\frac{p}{\rho} = RT \frac{\sum_{i=1}^N \frac{x_i}{M_i}}{\sum_{i=1}^N X_i M_i} = \frac{RT}{\sum_{i=1}^N X_i M_i} \quad (4)$$

where R is the universal gas constant, T is the temperature, N is the number of species in the mixture,  $x_i$  is the mass fraction of species i,  $X_i$  is the mole fraction of species i and  $M_i$  is the molecular weight of species i.

The temperature T is related to the mixture enthalpy h via the caloric equation of state

$$h = \sum_{i=1}^N x_i \left[ h_{f_i} + \int_{T_{f_i}}^T c_{p_i}(s) ds \right] \quad (5)$$

where  $h_{f_i}$  is the formation enthalpy of species i at the temperature  $T_{f_i}$ , and where  $c_{p_i}$  is the specific heat at constant pressure of species i. Values of  $h_{f_i}$  and  $T_{f_i}$ , and empirical relations between  $c_p$  and T for different species can be found in Refs. 9 and 10.

To complete the set of equations (1) - (5), formulas are needed for the mixture viscosity  $\mu$  (which appears in the stress tensor) and the mixture thermal conductivity k (which appears in the heat flux vector). By Wilke's semi-empirical formula (Ref. 11),

$$\mu = \frac{\sum_{i=1}^N \frac{X_i \mu_i}{\sum_{j=1}^N X_j \Phi_{ij}}}{\sum_{j=1}^N X_j \Phi_{ij}} \quad (6)$$

where  $\mu_i$  is the viscosity of species i, and where  $\Phi_{ij}$  is given by

$$\Phi_{ij} = \frac{1}{8^{\frac{1}{2}}} \left( 1 + \frac{M_i}{M_j} \right)^{-\frac{1}{2}} \left[ 1 + \left( \frac{\mu_i}{\mu_j} \right)^{\frac{1}{2}} \left( \frac{M_j}{M_i} \right)^{\frac{1}{4}} \right]^2 \quad (7)$$

The viscosity of a single species can be determined from the kinetic theory expression (Refs. 12, 13)

$$\mu_{\text{single species}} = 266.93 \cdot 10^{-7} \frac{(MT)^{\frac{1}{2}}}{\sigma^2 \Omega_V} \quad (8)$$

where  $\mu$  is given in g/cm-s, T in K, and where  $\sigma$  is a molecular collision diameter (in Angstrom), and  $\Omega_V$  is a viscosity collision integral, which can be approximated by (Ref. 14)

$$\Omega_V \approx 1.147 \left[ \frac{T}{T_\epsilon} \right]^{-0.145} + \left[ \frac{T}{T_\epsilon} + 0.5 \right]^{-2} \quad (9)$$

Here  $T_\epsilon$  is a molecular temperature diameter. Values for  $\sigma$  and  $T_\epsilon$  can be found in Ref. 15.

Finally, the thermal conductivity k is given by Eucken's approximation (Ref. 13),

$$k = \sum_{i=1}^N \frac{X_i k_i}{\sum_{j=1}^N X_j \Phi_{ij}} \quad (10)$$

where  $k_i$  is the thermal conductivity of species i,

$$k_i \approx \left( C_{pi} + \frac{5}{4} \frac{R}{M_i} \right) \mu_i \quad (11)$$

and where  $\Phi_{ij}$  is the same function as in Eqs. (6) - (7).

At M=15 and 250 kft altitude, the freestream Reynolds number per foot is  $3.5 \times 10^3$ . Flight experiments give the transition Reynolds number on cones at these Mach numbers as being in excess of  $10^6$ , so for conical bodies the transition region will begin in the wake and laminar flow may be assumed. At lower altitudes, say around 100 kft, the transition region from laminar to turbulent flow would begin around one foot and, depending on the type of vehicle, it would be necessary to consider turbulent flow over the body at these altitudes. This potential development has been kept in mind, but for the present, only laminar flow is considered.

The radiation source term in the energy equation (3) has to be obtained from a radiation transport model. Since the primary focus of the Phase I effort has been the chemically reacting phenomena, the radiation term has not been included

yet. Under the proposed Phase II effort, radiation models would be reviewed and an appropriate one would be chosen for incorporation into the code.

In summary, the system of equations used in the present effort consists of the partial differential equations (1) - (3) and the auxiliary relations (4) - (11). Given the mole fractions of each of the species of the mixture (or, equivalently, given the mass fractions), these equations can be solved for the mixture properties  $\rho$ ,  $U$ ,  $h$ ,  $p$ , and  $T$ .

The numerical method used to solve the system of equations is based on the finite difference approach discussed by Briley and McDonald (Refs. 16, 17), which uses a consistently split, linearized block-implicit (LBI) ADI procedure. The LBI scheme, being an implicit method, does not suffer from the stability restrictions which relate the temporal step to the spatial mesh size. This is an important advantage in view of the existence of high characteristic velocities, and the need to use locally refined meshes for accurate prediction of the flow field near solid surfaces, and in the regions of sharp temperature or species concentration gradients. Further, the solution procedure treats the nonlinearities noniteratively by Taylor series linearization to the requisite order in time, and then splitting the matrix into a series of easily solved block-banded subsystems. The solution procedure is, thus, computationally efficient. Further details on the LBI algorithm are available in Refs. 16 and 17.

During the Phase I effort, the existing scheme for the solution of equations (1) - (3) for a single species has been augmented by the relations (4) - (11) to allow the solution of equations (1) - (3) for a gas mixture, given the mass fractions (or mole fractions) of each of the species in the mixture.

### 3.2. Step 2 - The Species Transport Phase

In the species transport phase, each species is represented in each cell by a number of computational particles. A computational particle can be thought of as a collection of molecules of the same species that have the same velocity. Each computational particle is then moved over a time step using a convection velocity computed in the continuum phase, and an appropriate diffusion velocity. In the DSMC method, this diffusion velocity is obtained using a molecular velocity distribution function (such as a Maxwellian distribution function), and collisions between the "groups of molecules" are carried out at the end of each time step.

In the present approach, a macroscopic diffusion velocity is used, rather than a molecular one, and no collisions take place between the computational particles. The macroscopic properties that result from the collision procedure in the DSMC method, such as the viscosity and the species diffusivity into the mixture, are computed explicitly, and the motion of the computational particles is used to simulate the solution of the species convection-diffusion equations by means of a probabilistic method. The advantage of the present approach is that a larger time step can be used than the one required in the DSMC method.

The two aspects of the species transport phase that need to be discussed are (a) the computation of the macroscopic diffusion velocity and (b) the numerical scheme for moving the computational particles.

The macroscopic diffusion velocity of a particle is obtained by randomly picking velocity components from a Gaussian distribution  $f(\xi)$  with zero mean and standard deviation  $(2D\Delta t)^{1/2}$ ,

$$f(\xi) = \frac{1}{2(\pi D\Delta t)^{1/2}} e^{-\xi^2/(4D\Delta t)} \quad (12)$$

where  $\Delta t$  is the time step over which the particle has to be moved, and where  $D$  is the diffusivity of the species under consideration into the mixture. This result follows from the requirement that the motion of a large number of particles leads to a particle distribution (i.e. species concentration distribution) that is consistent with the solution of the diffusion equation for the species under consideration (see, for example, Refs. 18 and 19). The diffusivity  $D_i$  of the species  $i$  into the mixture can be determined from the relation (Ref. 13)

$$D_i \approx \frac{1 - X_i}{\sum_{\substack{j=1 \\ j \neq i}}^N \left[ \frac{X_j}{D_{ij}} \right]} \quad (13)$$

where  $D_{ij}$  is the binary diffusion coefficient of species  $i$  into species  $j$ , which can be expressed as

$$D_{ij} = \frac{0.001858 T^{3/2} \left[ \frac{1}{M_i} + \frac{1}{M_j} \right]^{1/2}}{p \sigma_{ij}^2 \Omega_D} \quad (14)$$

Here  $D_{ij}$  is in  $\text{cm}^2/\text{s}$ ,  $p$  in atm,  $T$  in K, and  $\sigma_{ij}$ , the effective collision diameter given by  $\sigma_{ij} = \frac{1}{2}(\sigma_i + \sigma_j)$ , where  $\sigma_i$  is the molecular collision diameter of species  $i$ , in Å. The diffusion collision integral  $\Omega_D$  can be approximated by (Ref. 14).

$$\Omega_D \approx \left[ \frac{T}{T_{\epsilon ij}} \right]^{-0.145} + \left[ \frac{T}{T_{\epsilon ij}} + 0.5 \right]^{-2.0} \quad (15)$$

where

$$T_{\epsilon ij} = \left[ T_{\epsilon i} T_{\epsilon j} \right]^{1/2} \quad (16)$$

( $T_{\epsilon i}$  being the molecular temperature diameter of species  $i$ ). The values of  $\sigma$  and  $T_{\epsilon}$  used in the computation of the diffusivities via Eqs. (14) - (16) are the same as those used in the computation of the viscosities via Eqs. (8) - (9). Once the proper diffusivity  $D$  has been computed using Eqs. (13) - (16), diffusion velocity components can be picked from the distribution (12), and the particle velocity is obtained by adding the diffusion velocity to the convection velocity as computed in the continuum phase.

The numerical scheme used to move the computational particles is based on the particle transport model incorporated into the CELMINT (Combined Eulerian Lagrangian Multidimensional Implicit Navier-Stokes Time-Dependent) code developed for the computation of flows that contain solid particles or liquid droplets (Ref. 20). The key feature of this particle transport model is that it integrates the Lagrangian equations of motion for a particle in computational space rather than physical space. This eliminates the need to search for the mesh cell in which a particle resides. The present application of this model differs from the previous applications of the SRA code (Refs. 21, 22) in that there is no force acting on the computational particle. The equation of motion is, in this case,

$$\frac{d\mathbf{x}}{dt} = \mathbf{v} \quad (17)$$

where  $\mathbf{x}$  is the position vector of the particle, and  $\mathbf{V}$  is the particle velocity. In computational space, this equation becomes

$$\frac{dy^i}{dt} = \sum_{j=1}^3 \frac{\partial y^i}{\partial x_j} V_j \quad (i = 1, 2, 3) \quad (18)$$

where  $y^i$  are the computational coordinates,  $x_i$  are the physical coordinates (the components of  $\mathbf{x}$ ), and  $V_i$  are the physical velocity components (the components of  $\mathbf{V}$ ) of the particle.

Integration of Eq. (18) allows tracking of the particle motion in the computational space. As mentioned above, this eliminates the need to search for the mesh cell in which a particle resides. In addition, this simplifies the search for boundaries, needed to determine whether a particle has reached a solid boundary and should be reflected, or a particle has left the computational domain altogether and should be omitted. As a consequence, the method can be applied easily to particle motion in rather complex geometries (Ref. 22).

In summary, the species transport phase consists of the following steps:

- (i) Given the mass fractions (or mole fractions) of each of the species in a mesh cell, the number of computational particles of each species in each cell is determined.
- (ii) The computational particles are distributed randomly across the mesh cell.
- (iii) Each particle is moved over a time step using a mixture convection velocity computed in the continuum phase, and a diffusion velocity randomly picked from a distribution based on the species dispersion into the mixture (Eqs. 12-16).

At the end of the species transport phase, a new distribution of computational particles is obtained, to be used in the reaction phase, described below.

### 3.3 Step 3 - The Chemical Reaction Phase

In the reaction phase, a representative set of reactions that takes place in the time interval  $\Delta t$  is computed among computational particles by means of techniques similar to those used in DSMC methods. Since the choice of molecular

collision/reaction models is an important aspect of the DSMC methods, a brief history is presented first.

Early applications of the direct simulation methods employed the well established models of classical kinetic theory (Refs. 12, 23). The hard sphere model is the easiest to apply, and both it and the Maxwell model were widely used for early studies in which the primary objective was to make comparisons with other numerical or analytical methods employing the same model. These models are associated with unrealistic viscosity-temperature power laws and became inadequate when serious comparisons were to be made with experiment. The structure of strong shock waves was the subject of the first serious comparisons of DSMC results and experiment. The inverse power law of repulsion model was first implemented (Ref. 24) and some calculations were made (Ref. 25) with the  $\text{Exp}^{-6}$  and Lennard-Jones models that include the long range attractive force. The simpler model was found to be generally adequate for engineering studies. In all the successful correlations between experiment and simulation, the molecular impact parameters were chosen to match the coefficient of viscosity of the real gas.

Experience was gradually accumulated on the effects of the molecular model on representative flows. It was found that the observed effects could be fully correlated with the variation, due to their relative velocity in the collision, of the differential cross-section of the molecules. The form of the deflection angle scattering law of the molecules appeared to be comparatively unimportant. These considerations led to the introduction (Ref. 26) of the variable hard sphere, or VHS, molecular model. This is essentially a hard sphere with a diameter that varies as some inverse power of the relative velocity in the collision. The VHS model is the simplest one that is capable of modeling the viscosity coefficient, including its temperature dependence, of real molecules. It has been found (Refs. 27, 18) that, as long as this is done, the results are independent of the molecular model.

Nonequilibrium chemical reactions are readily handled by procedures that are essentially extensions of the elementary collision theory of chemical physics. In this, the binary reaction rate is obtained as the product of the collision rate for collisions with energy in excess of the activation energy and the probability of reaction or steric factor. Since the formulation is in terms of kinetic theory, the model can be incorporated directly into the DSMC method.

The chemical data for gas phase reactions is almost invariably quoted in terms of the reaction rate constant. A form of the collision theory that is consistent

with the VHS model can be used (Ref. 7) to convert the temperature dependent rate constants of continuum theory into collision energy dependent steric factors of reaction cross-sections. Alternatively, the reactive cross-sections may be available directly from the thermophysical database (Refs. 1, 5, 6, 25). While this is more in keeping with the simulation approach, it leads to increased difficulties in ensuring that the data for the forward and reverse reactions is consistent with chemical equilibrium in situations where the reactions should proceed to equilibrium. Extensive calculations have been made (Ref. 4) for the atmospheric reentry of the Space Shuttle and direct comparisons were made with flight data and with overlapping continuum calculations. Recombination reactions are not important at very low densities where the probability of three-body collisions is extremely small. They become important in the continuum overlap region and these are dealt with by assigning a lifetime to each binary collision and regarding the ternary collision as a further binary collision between the pair of molecules in the original collision and a third molecule. These procedures can be incorporated into the DSMC method in a form (Ref. 29) that guarantees the correct equilibrium state.

The present approach follows the procedure described by Bird (Ref. 7), which uses the VHS molecular model and reaction cross-sections that are based on the (temperature dependent) rate constants of continuum theory. The numerical scheme consists of the following steps (for each mesh cell):

- (i) Pick a reaction among the set of all binary reactions under consideration, say  $A + B \rightarrow C + D$ .
- (ii) Pick one particle of each of the (two) species A and B. Note that the statistical weight of these particles (i.e. the number of physical molecules that they represent) must be the same. In the DSMC method, the particles chosen have velocities associated with them. In the present method, the choice of a particle includes the choice of velocity components from the appropriate (for example, Maxwellian) molecular velocity distribution.
- (iii) Determine the reaction cross-section.

- (iv) Based on the reaction probability, which relates directly to the reaction cross-section, determine whether or not a reaction takes place.
- (v) If a reaction takes place, create particles of the species C and D, and omit the particles of species A and B. In other words, update the species concentrations. In addition, update a reaction time counter by an amount inversely proportional to the reaction probability.
- (vi) Omit the reaction from the set of reactions under consideration if its time counter exceeds the physical time.
- (vii) Repeat the procedure until the set of reactions is empty, i.e. until all reaction time counters have exceeded the physical time.

The use of reaction time counters ensures that, over a large number of reactions, the procedure leads to a reaction rate that is in agreement with the reaction cross-section (cf. Ref. 7). This leads to an interesting observation: if the reaction cross-sections are determined such that the resulting reaction rates correspond to those of continuum theory, then the steps (ii) - (v) in the above procedure could be replaced by

- (v)\* Let a reaction take place. Update the species concentrations; update the reaction time counter by an amount inversely proportional to the reaction rate.

In that case, the procedure can be considered as a stochastic method for solving a system of ordinary differential equations of the form

$$\frac{dn_A}{dt} = -\sum_B n_A n_B k_{AB}(T) + \sum_{C,D} n_C n_D k_{CD}(T) \quad (19)$$

where  $n_A$  denotes the number density of species A, and  $k_{AB}(T)$  and  $k_{CD}(T)$  are the (continuum) rate coefficients. The first sum on the right-hand side of Eq. (19) is over all reaction of the form  $A + B \rightarrow \dots$ , while the second sum is over all reactions of the form  $C + D \rightarrow A + \dots$

The advantage of using the complete procedure (i) - (vii) rather than the simplified one (with (ii) - (v) replaced by (v)\*) lies in the fact that alternative formulations for the reaction cross-sections, based on molecular models rather than continuum theory, can be implemented easily.

#### 3.4. Coupling of the Three Phases

Finally, it is necessary to make some remarks about the coupling of the three phases in the hybrid scheme developed under the present effort. The continuum phase provides the species transport phase with a convection velocity and with mixture properties that are used to compute the diffusion velocity. The species mass fractions (or mole fractions), which are not changed by the continuum phase, and the mixture density provide the species number densities, used to determine the number of computational particles of each species and their statistical weights.

The species transport phase moves the computational particles, thereby updating the species number densities in each mesh cell. The chemical reaction phase updates the number densities once more when reactions take place. This phase also uses some continuum properties (such as temperature) in the computation of reaction cross-sections. At the end of the reaction phase, new species mass fractions (or mole fractions) can be computed in each mesh cell. As such, the combined transport/reaction phase serves to update only the species mass fractions.

A word of caution is necessary here. The species mass fractions that are computed at the end of the combined transport/reaction phase make sense in the continuum phase only if a very large number of computational particles is used, or, equivalently, if an ensemble average is taken over a large number of separate calculations. Since for steady-state calculations a time-average is equivalent to an ensemble average, it is advantageous to reduce the number of particles used in each time step, and to time-average the mass fractions computed by the transport/reaction phase before they are used in the continuum phase. Due to the coupling of the continuum phase and the transport/reaction phase this cannot be done efficiently directly, but as can be shown, the required averaging can be accomplished via underrelaxation of the changes in the species mass fractions before they are used in the continuum phase.

#### 4. RESULTS AND CONCLUSIONS

The hybrid approach described above has been developed under the Phase I program. In order to demonstrate the feasibility of this approach, a calculation has been performed for the axisymmetric hypersonic laminar flow of dissociating air over a 10 - degree cone. Although this represents a relatively simple test case chosen to clarify the evaluation of the procedure, it does contain all the basic elements of hypersonic vehicle environment simulation insofar as they have been included in the present model.

The relevant flow conditions for the test case are:

Altitude	45.72 km (150 kft)
Velocity	3.27 km/s (10.73 kft/s)
Mach Number	10
Ambient Pressure	136.7 N/m <sup>2</sup>
Ambient Temperature	266.2 K
Ambient Mole Fractions:	
O <sub>2</sub>	0.24
N <sub>2</sub>	0.76

The wall was assumed adiabatic and non-catalytic. The chemical reactions considered in the present study consist of 19 reactions for 5 species (N<sub>2</sub>, O<sub>2</sub>, NO, N and O), and the data are listed in Table 1, which was taken from Ref. 30. Three-body atom recombination reactions are not significant at high altitudes, and have not been included.

Figure 1 shows the computational domain and the numerical grid used in the calculations. The downstream boundary of the computational domain (boundary DE in Fig. 1) is about 3 inches from the vertex of the cone (point C), to ensure laminar flow over the section CD of the cone under consideration. The upstream boundary AB and the "far-field" boundary AE were chosen such that they were both inflow boundaries. The bow shock wave intersects the downstream boundary. The grid used contains 100 × 150 mesh points, concentrated near the cone surface and the cone vertex, to allow proper resolution of the boundary layer.

Results of the computation are shown in Figures 2-8. Figure 2 shows contours of the density, the pressure, and the temperature. In this figure, the shock wave and the boundary layer can be distinguished easily. The location and strength of

the bow shock are in good agreement with the inviscid theory of conical flow, even though no particular attention was paid to resolving the bow shock. As can be seen in Figure 2b, the pressure is approximately constant across the boundary layer. In Figures 3-5, the temperature calculated for the reacting flow is compared with the temperature that can be obtained for non-reacting flow, without species transport, i.e. for the flow with "frozen" species concentrations. Figure 3 shows that the temperature on the cone surface is lower for the reacting flow than for the non-reacting flow. This effect is to be expected, because the formation of O, NO, and N requires energy. The high temperature calculated near the cone vertex indicates that the flow near this vertex has been resolved adequately. In Figure 4, the temperature profile is shown at an axial distance of 2.5 inches downstream of the cone vertex. The thickness of the shock indicates a lack of grid resolution in the shock wave. Again, the temperature of the reacting flow is seen to be lower than the temperature of the non-reacting flow. Figure 5a is an enlargement of Figure 4 in the boundary layer region, while Figures 5b-c show the temperature profiles at axial distances of 1.0 and 0.1 inch downstream of the cone vertex.

Figure 6 shows contours of the mass fractions of O, NO, and N in the region from 2.0 to 2.5 inches downstream of the cone vertex. The mass fractions can be seen to increase in the axial direction because O, NO and N are not only produced by the chemical reactions, but also convected downstream by the mean flow. The increase of the mass fractions along the cone surface is also clearly visible in Figure 7. Finally, Figure 8 shows profiles of the mass fractions at several axial locations.

The results of the calculation discussed above demonstrate that the hybrid scheme is capable of computing chemically reacting flows and has the potential for efficiently computing high Mach number flows around vehicles in the upper layers of the atmosphere. Further development of this scheme is the focus of the proposed Phase II effort.

Table 1. List of Chemical Reactions.

Five-species Model.<sup>a</sup>

Number	Reaction	Rate Coefficient, in m <sup>3</sup> /molecule-s		
		a	b	c
1	O <sub>2</sub> + N → 2O + N	5.993×10 <sup>-12</sup>	-1.0	59370
2	O <sub>2</sub> + NO → 2O + NO	5.993×10 <sup>-12</sup>	-1.0	59370
3	O <sub>2</sub> + N <sub>2</sub> → 2O + N <sub>2</sub>	1.198×10 <sup>-11</sup>	-1.0	59370
4	O <sub>2</sub> + O <sub>2</sub> → 2O + O <sub>2</sub>	5.393×10 <sup>-11</sup>	-1.0	59370
5	O <sub>2</sub> + O → 2O + O	1.498×10 <sup>-10</sup>	-1.0	59370
6	N <sub>2</sub> + O → 2N + O	3.187×10 <sup>-13</sup>	-0.5	113000
7	N <sub>2</sub> + O <sub>2</sub> → 2N + O <sub>2</sub>	3.187×10 <sup>-13</sup>	-0.5	113000
8	N <sub>2</sub> + NO → 2N + NO	3.187×10 <sup>-13</sup>	-0.5	113000
9	N <sub>2</sub> + N <sub>2</sub> → 2N + N <sub>2</sub>	7.968×10 <sup>-13</sup>	-0.5	113000
10	N <sub>2</sub> + N → 2N + N	6.900×10 <sup>-8</sup>	-1.5	113000
11	NO + N <sub>2</sub> → N + O + N <sub>2</sub>	6.590×10 <sup>-10</sup>	-1.5	75550
12	NO + O <sub>2</sub> → N + O + O <sub>2</sub>	6.590×10 <sup>-10</sup>	-1.5	75550
13	NO + NO → N + O + NO	1.318×10 <sup>-8</sup>	-1.5	75550
14	NO + O → N + O + O	1.318×10 <sup>-8</sup>	-1.5	75550
15	NO + N → N + O + N	1.318×10 <sup>-8</sup>	-1.5	75550
16	NO + O → O <sub>2</sub> + N	5.279×10 <sup>-21</sup>	1.0	19700
17	N <sub>2</sub> + O → NO + N	1.120×10 <sup>-16</sup>	0.0	37500
18	O <sub>2</sub> + N → NO + O	1.598×10 <sup>-18</sup>	0.5	3600
19	NO + N → N <sub>2</sub> + O	2.490×10 <sup>-17</sup>	0.0	0

<sup>a</sup> Without three-body recombination reactions which do not participate at low densities.

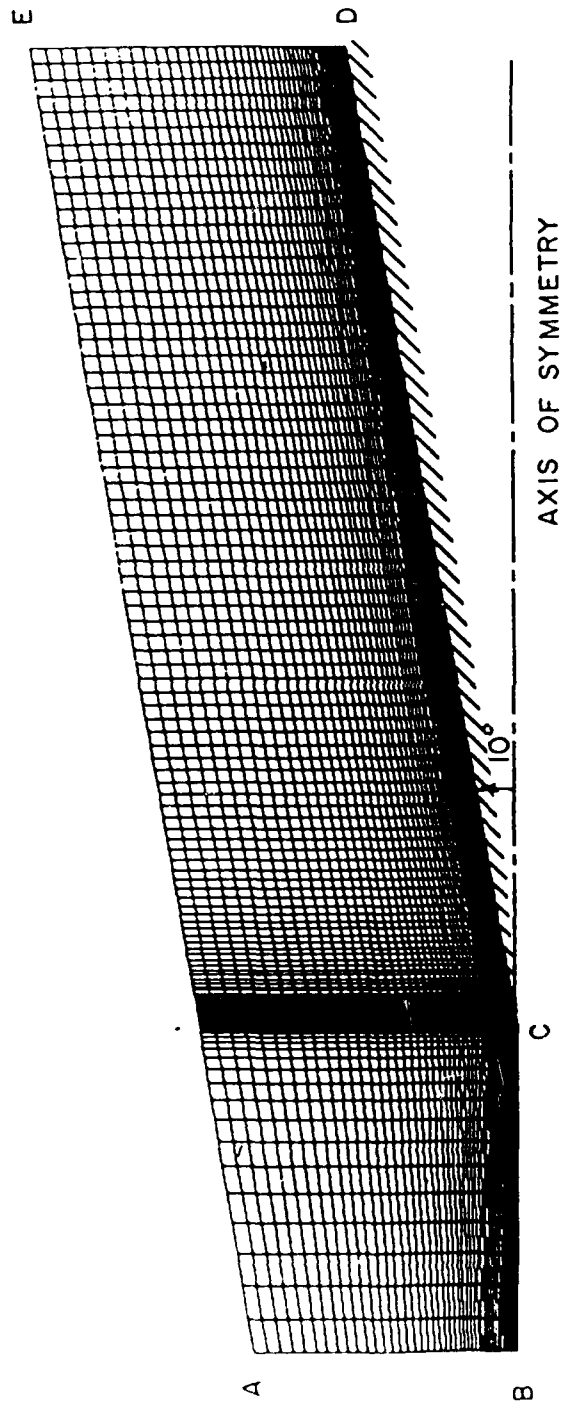
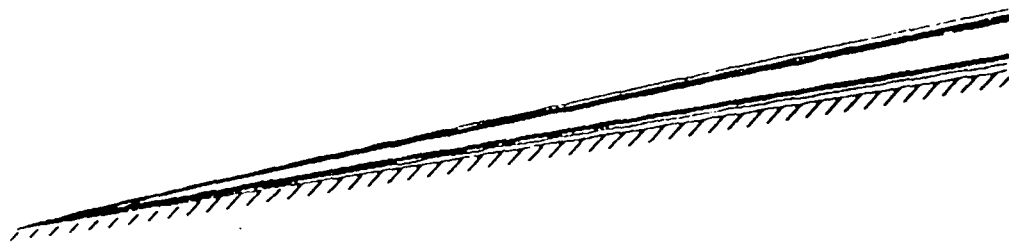
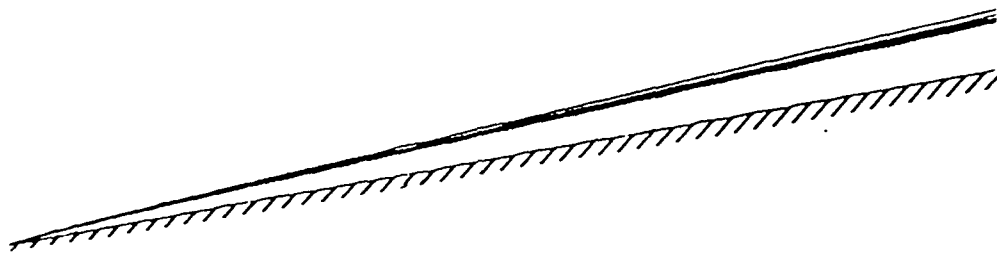


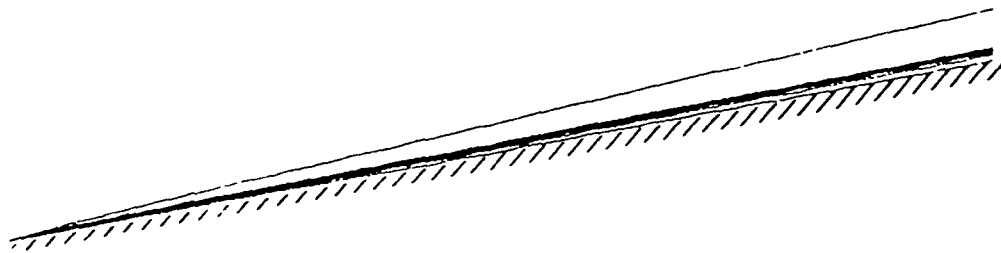
Figure 1. Computational Domain and Grid



(a) Density



(b) Pressure



(c) Temperature

Figure 2. Contours of Density, Pressure, and Temperature  
Between  $x = 0$  and  $x = 3$

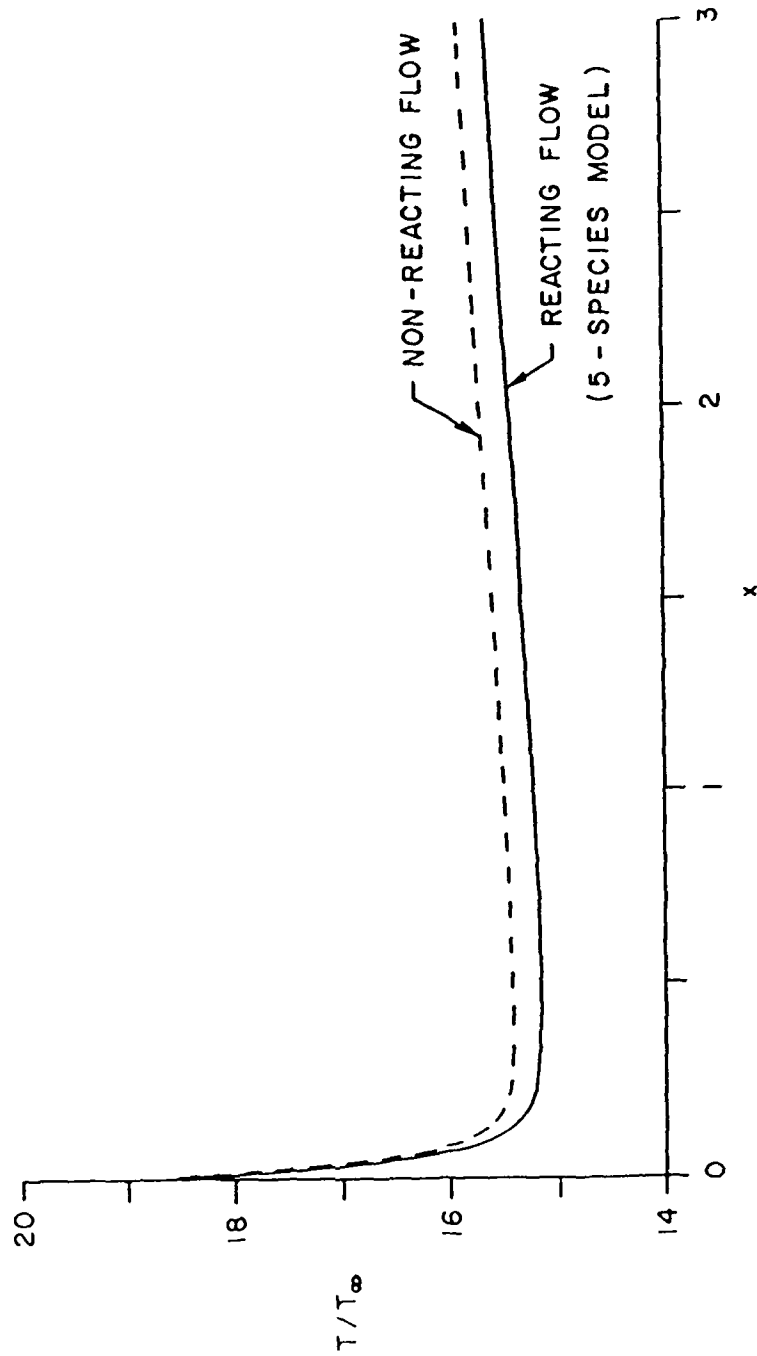


Figure 3. Axial Variation of the Temperature Along the Cone Surface

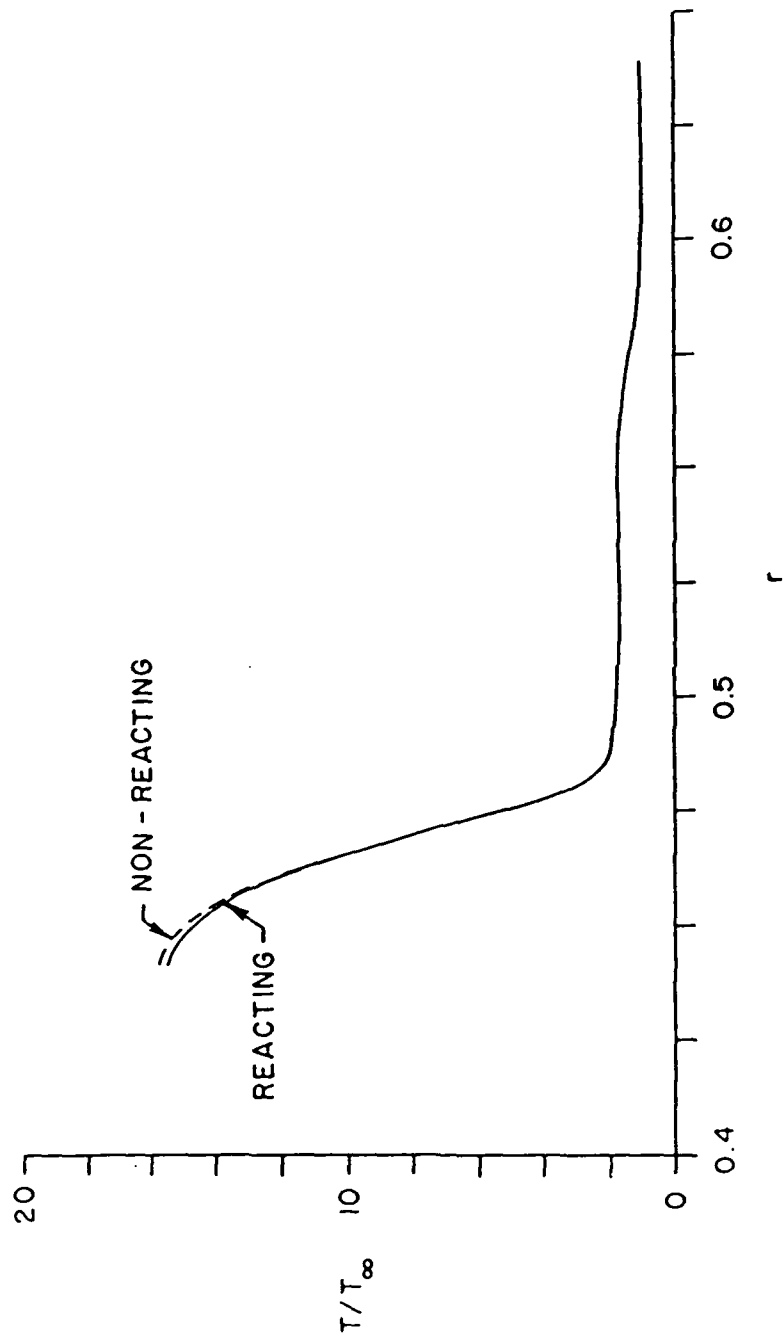


Figure 4. Radial Variation of the Temperature at  $x = 2.5$

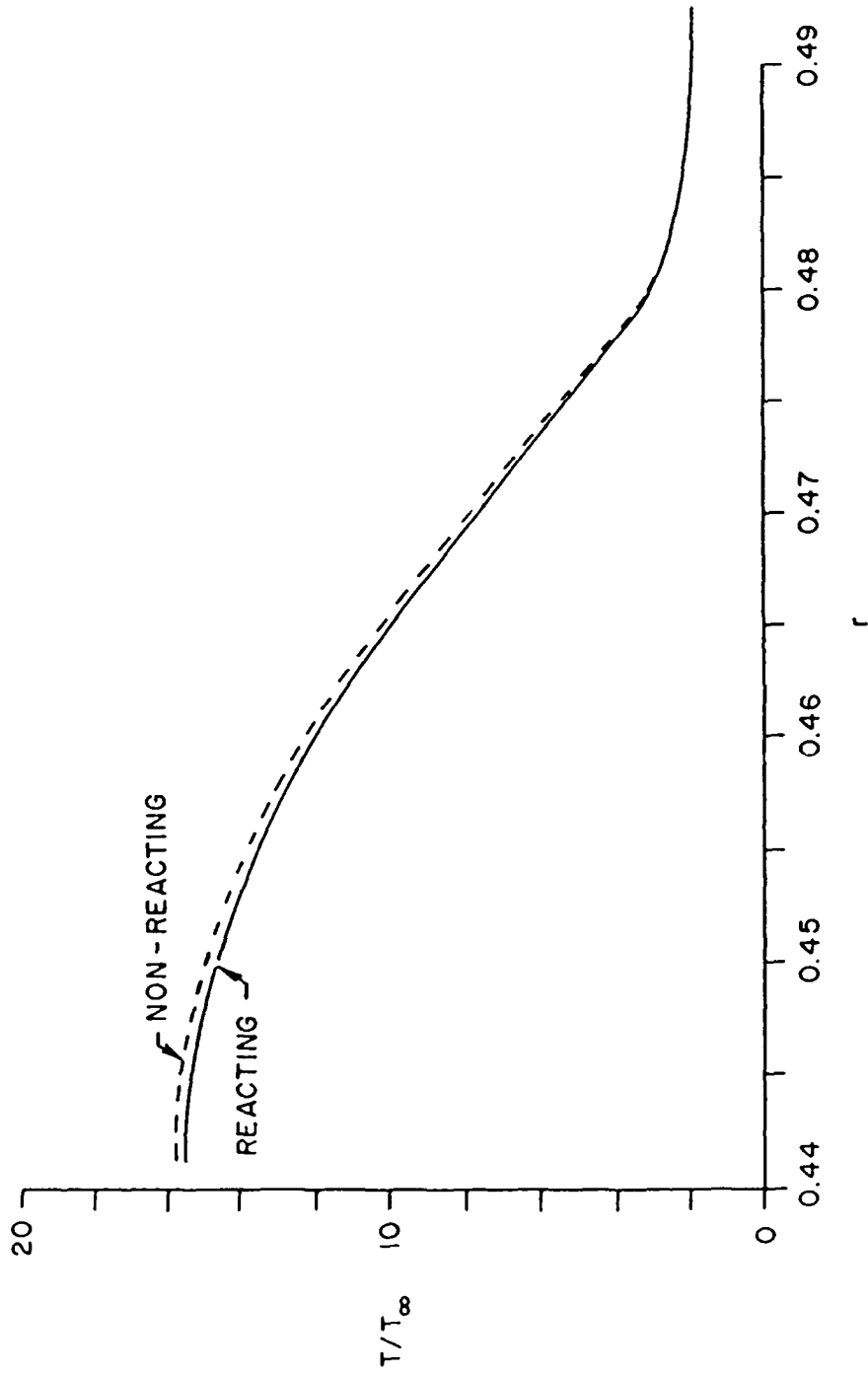


Figure 5a. Radial Variation of the Temperature at  $x = 2.5$

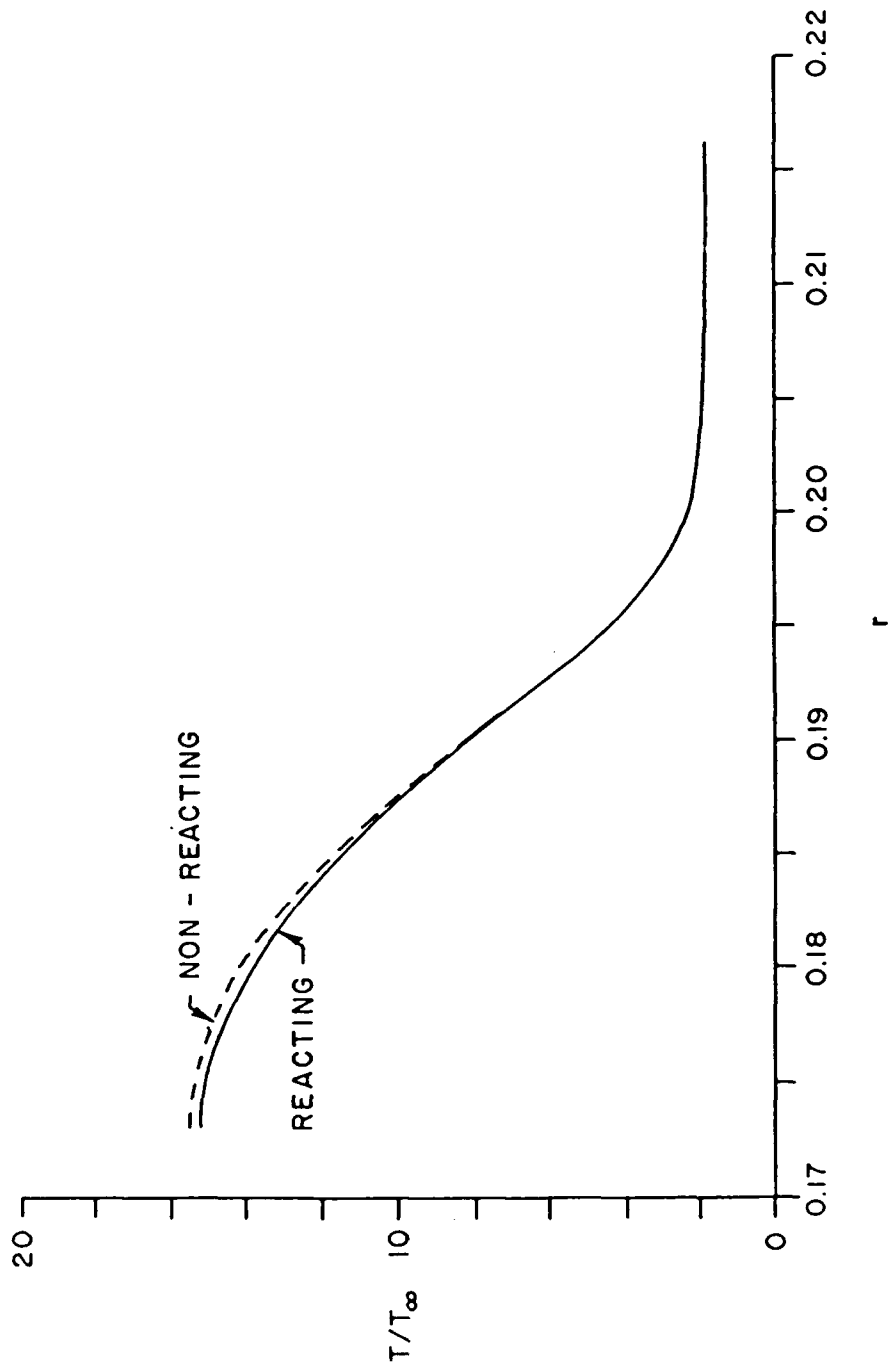


Figure 5b. Radial Variation of the Temperature at  $x = 1.0$

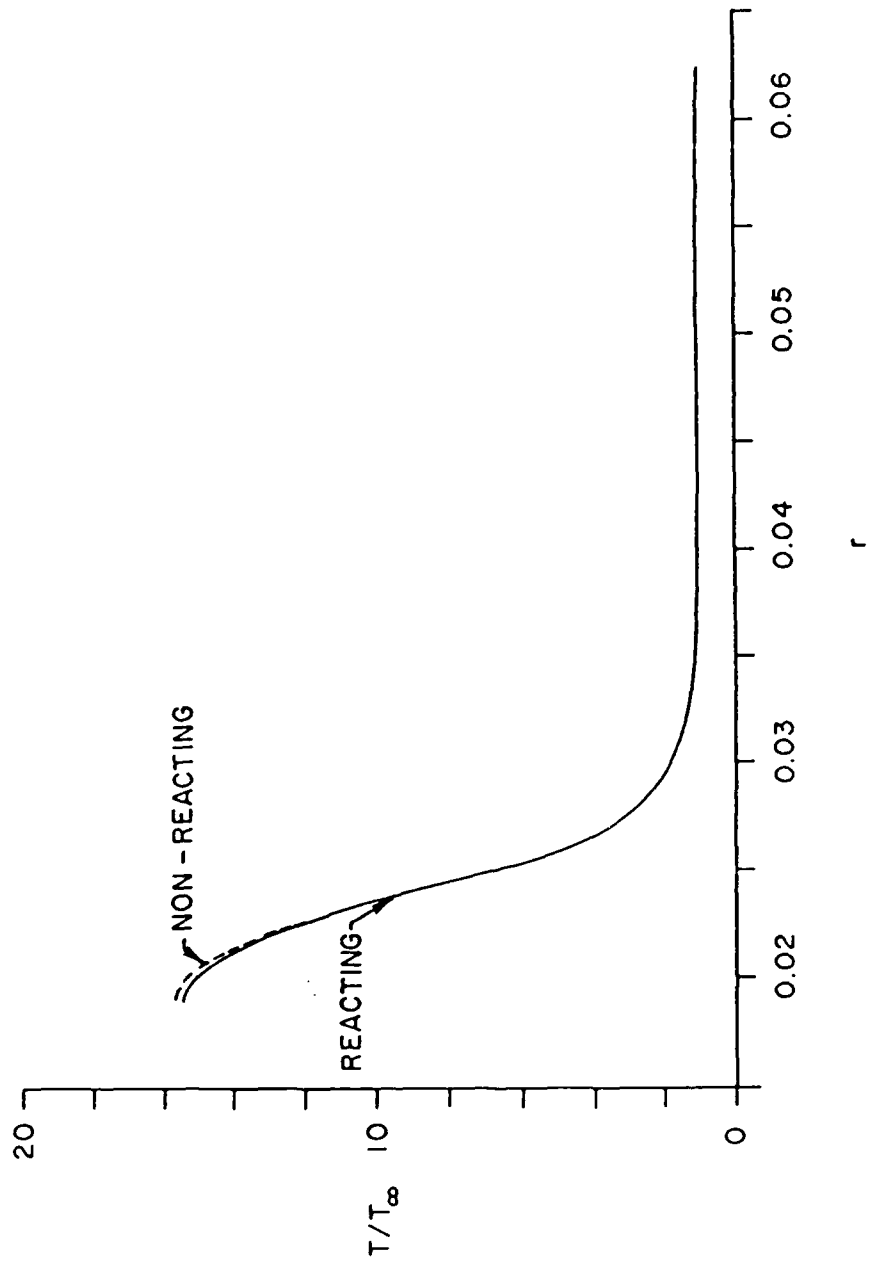
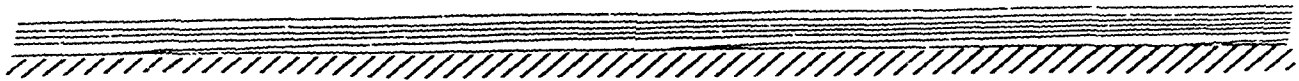


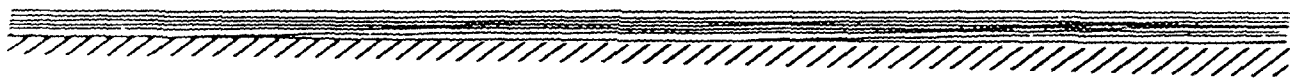
Figure 5c. Radial Variation of the Temperature at  $x = 0.1$



(a) O Mass Fraction



(b) NO Mass Fraction



(c) N Mass Fraction

Figure 6. Contours of the Mass Fractions of O, NO, and N  
Between  $x = 1.85$  and  $x = 2.60$

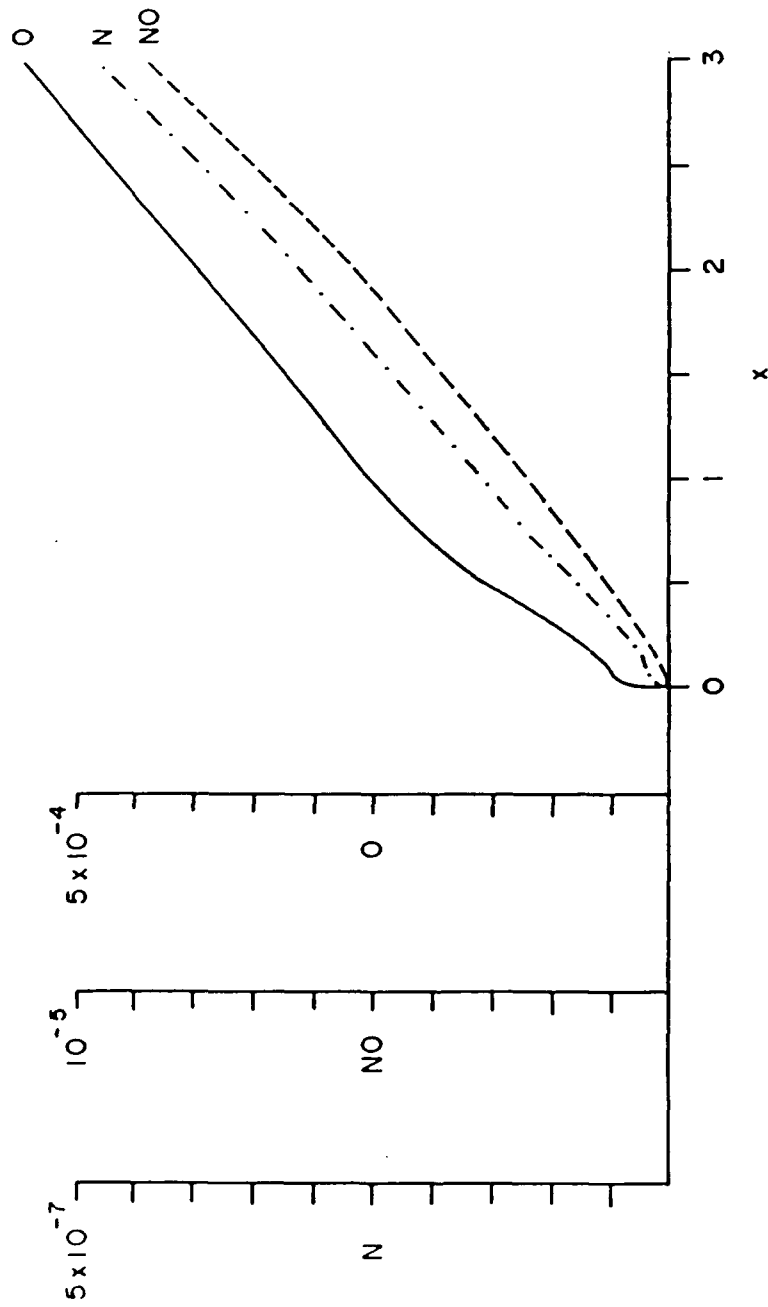


Figure 7. Axial Variation of the Mass Fractions Along the Cone Surface

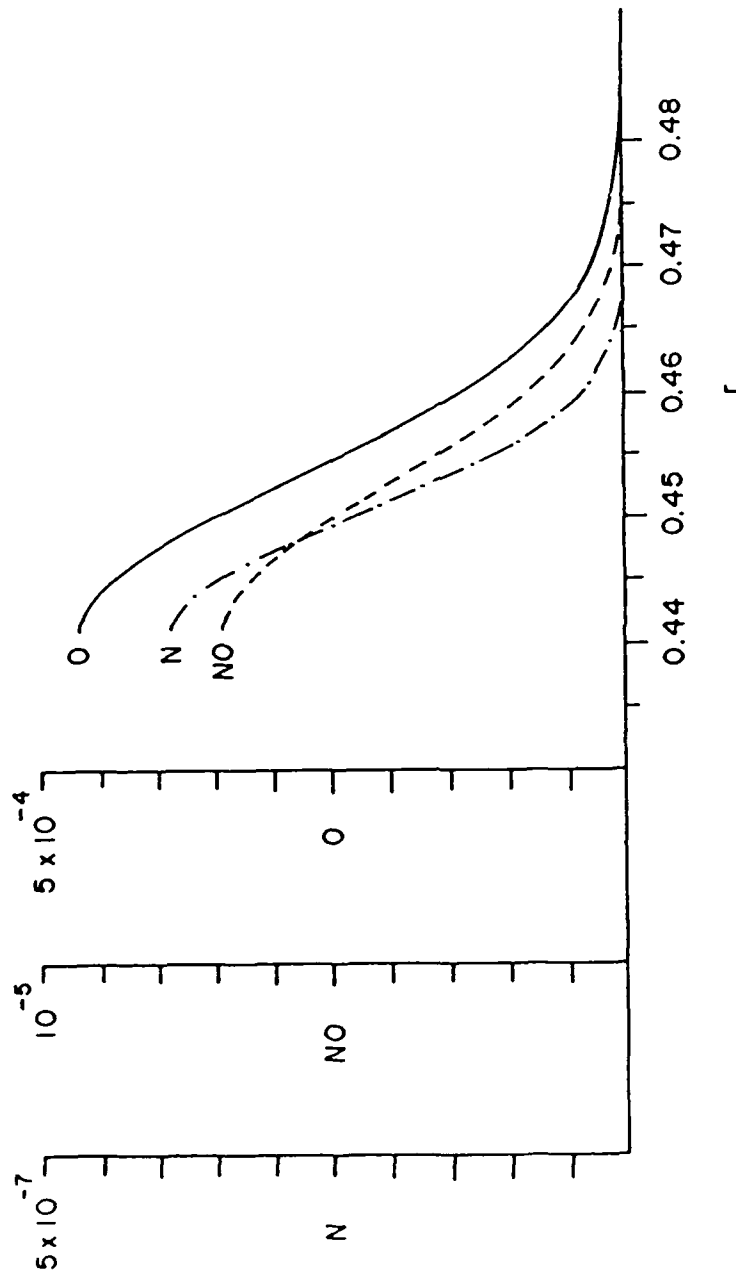


Figure 8a. Radial Variation of the Mass Fractions at  $x = 2.5$

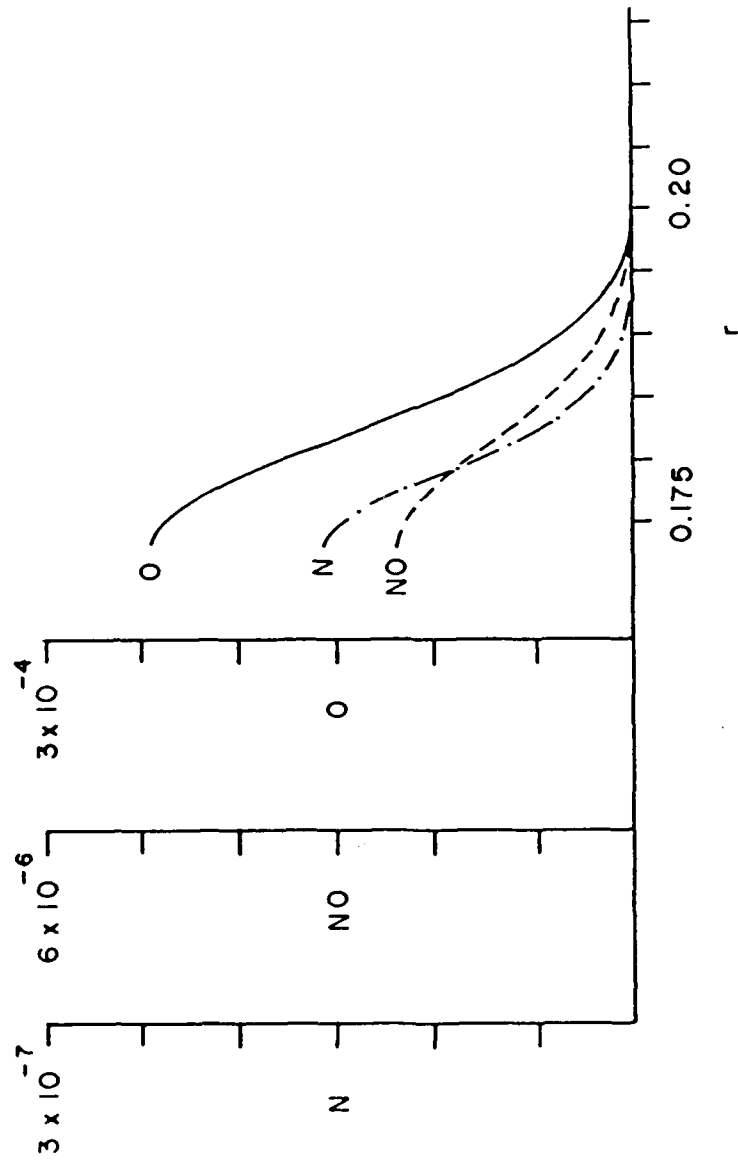


Figure 8b. Radial Variation of the Mass Fractions at  $x = 1.0$

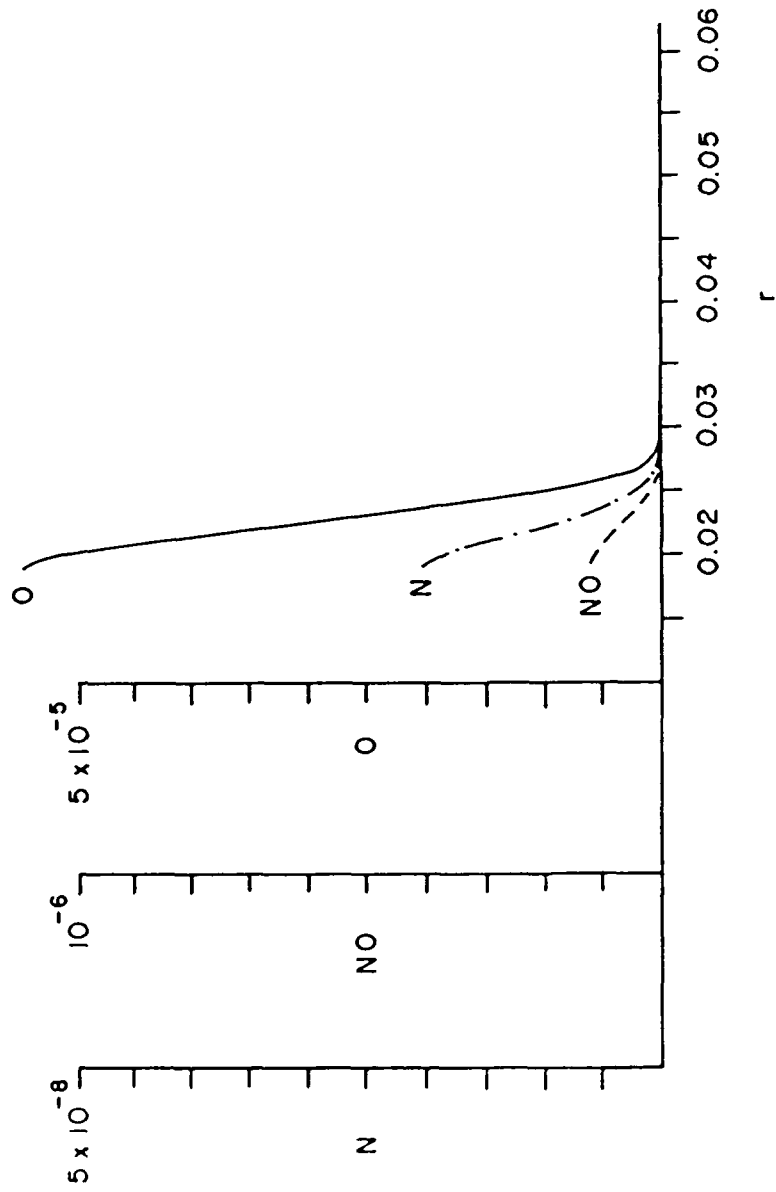


Figure 8c. Radial Variation of the Mass Fractions at  $x = 0.1$

## 5. FUTURE DEVELOPMENT

As described above, under the Phase I effort a hybrid Navier-Stokes/Monte Carlo method has been developed for the computation of hypersonic, viscous, chemically reacting flows. This method consists of three major phases. The first phase is the continuum phase where the mean flow field calculations are performed via numerical solution of the Navier-Stokes equations and the global continuity and energy equations for the gas mixture. The second phase is the species transport phase, where the "computational particles" representing the species molecules are transported simulating the convection and diffusion of the species. Finally, the third phase is the reaction phase, where appropriate collision models are used in a Monte Carlo-like way to simulate the chemical kinetics. The first phase uses an Eulerian description, while the second and third phases utilize a statistical Lagrangian description. The method offers the flexibility of the DSMC-method with respect to the chemical reactions, but allows the use of larger time steps, because molecular collision properties such as viscosity and diffusivity are obtained from semi-empirical relations.

A future effort would concentrate on the further development of both the numerical and the physical aspects of the hybrid scheme, with the objective of developing and demonstrating a computer code that can be used as a tool for investigating vehicle performance and sensor visibility in hypersonic flight within the atmosphere.

Specific tasks that would comprise this effort are the following:

- (i) Further development of the Lagrangian statistical species transport algorithm via the inclusion of sophisticated statistical models.
- (ii) Added capabilities in terms of boundary conditions (catalytic walls), recombination reactions, and ionization.
- (iii) Addition of a radiation transport model.
- (iv) Demonstration of the fully developed procedure via one or more relevant flow field calculations.

- (v) Development of suitable input and output packages for use of the code in a workstation environment.

These tasks have been detailed in a Phase II proposal.

## REFERENCES

1. Nelson, H.F. (Ed.): Thermal Design of Aeroassisted Orbital Transfer Vehicles, Progress in Astronautics and Aeronautics, Vol. 96, AIAA, New York, 1984.
2. Candler, G.V. and MacCormack, R.W.: The Computation of Hypersonic Flows in Chemical and Thermal Nonequilibrium, Paper No. 107, Third National Aero-Space Plane Technology Symposium, June 1987.
3. Green, M.J.: Numerical Simulation of Hypersonic, Axisymmetric Flowfields, AIAA Paper 86-1285, 1986.
4. Moss, J.N. and Bird, G.A.: Direct Simulation of Transitional Flow for Hypersonic Re-entry Conditions, Progress in Astronautics and Aeronautics, Vol. 96, AIAA, New York, 1984.
5. Shinn, J.L., Moss, J.N. and Simmonds, A.L.: Viscous Shock-Layer Heating Analysis for the Shuttle Windward Plane with Surface Finite Catalytic Recombination Rates, AIAA Paper 84-0842, AIAA/ASME 3rd Joint Thermophysics, Fluids, Plasma, and Heat Transfer Conference, St. Louis, Mo., June 1982.
6. Lee, J.H.: Basic Governing Equations for the Flight Regimes of Aeroassisted Orbital Transfer Vehicles, Progress in Astronautics and Aeronautics, Vol. 96, AIAA, New York, 1984.
7. Bird, G.A.: Molecular Gas Dynamics, Clarendon Press, Oxford, England, 1976.
8. Bird, G.A.: Monte Carlo Simulation of Multidimensional and Chemically Reacting Flows, Rarefied Gas Dynamics, Vol. 1, (R. Campargue, Ed.), CEA, Paris, 1979, pp. 365-388.
9. Benson, R.S.: Advanced Engineering Thermodynamics, Pergamon Press, Oxford, 1977.
10. JANNAF Thermochemical Tables, Dow Chemical Company, 1965.
11. Wilke, C.R.: A Viscosity Equation for Gas Mixtures, J. Computational Physics, Vol. 18, p. 517, 1950.
12. Hirschfelder, J.O., Curtiss, C.F. and Bird, R.B.: The Molecular Theory of Gases and Liquids, Wiley, New York, 1954.
13. Bird, R.B., Stewart, W.E., and Lightfoot, E.N.: Transport Phenomena, Wiley, New York, 1960.
14. White, F.M.: Viscous Fluid Flow, McGraw-Hill, New York, 1974.
15. Svehla, R.A.: Estimated Viscosities and Thermal Conductivities of Gases at High Temperatures, NASA Technical Report R-132, 1962.
16. Briley, W.R. and McDonald, H.: Solution of the Multidimensional Compressible Navier-Stokes Equations by a Generalized Implicit Method, J. Computational Physics, Vol. 24, pp. 372-397, 1977.

## REFERENCES

17. Briley, W.R. and McDonald, H.: On the Structure and Use of Linearized Block Implicit Schemes, *J. Computational Physics*, Vol. 34, 1980, pp. 547-73.
18. Monin, A.S. and Yaglom, A.M.: Statistical Fluid Mechanics, MIT Press, Cambridge, MA, 1973.
19. Hotchkiss, R.S.: The Numerical Modeling of Air Pollution Transport in Street Canyons, Report LA-UR-74-1427, Los Alamos Scientific Laboratory, 1974.
20. Sabnis, J.S., Gibeling, H.J. and McDonald, H.: A Combined Eulerian-Lagrangian Analysis for Computation of Two-Phase Flows, AIAA Paper No. 87-1419, AIAA 19th Fluid Dynamics, Plasma Dynamics and Lasers Conference, June 1987.
21. Sabnis, J.S., Choi, S.K., Buggeln, R.C. and Gibeling, H.J.: Computation of Two-Phase Shear Layer Flow Using an Eulerian-Lagrangian Analysis, AIAA Paper 88-3202, AIAA/ASME/SAE/ASEE 24th Joint Propulsion Conference, July 1988.
22. De Jong, F.J., Sabnis, J.S., and McConnaughey, P.K.: A Combined Eulerian-Lagrangian Two-Phase Analysis of SSME HPOTP Nozzle Plug Trajectories: Part I - Methodology, AIAA Paper 89-2347, AIAA/ASME/SAE/ASEE 25th Joint Propulsion Conference, July 1989 (to be presented).
23. Chapman, S. and Cowling, T.G.: The Mathematical Theory of Non-Uniform Gases, Cambridge University Press, London, 1952.
24. Bird, G.A.: Aspects of the Structure of Strong Shock Waves, *Phys. Fluids*, Vol. 13, pp. 1172-1177, 1970.
25. Sturtevant, B. and Steinhilper, E.A.: Intermolecular Potentials from Shock Structure Experiments, Rarified Gas Dynamics, (K. Karamcheti, Ed.) Academic Press, New York, pp. 159-166, 1974.
26. Bird, G.A.: Monte Carlo Simulation in an Engineering Context, Progress in Aeronautics and Astronautics, Vol. 74, pp. 239-255, 1981.
27. Bird, G.A.: Definition of Mean Free Path for Real Gases, *Phys. Fluids*, Vol. 26, pp. 3222-3223, 1983.
28. Bird, G.A.: Low Density Aerothermodynamics, AIAA Paper 85-0994, 1985.
29. Bird, G.A.: Direct Molecular Simulation of a Disassociating Diatomic Gas, *J. Computational Physics*, Vol. 25, p. 405, 1977.
30. Moss, J.N., Bird, G.A., and Dogra, V.K.: Nonequilibrium Thermal Radiation for an Aeroassist Flight Experimental Vehicle, AIAA Paper 88-0081, AIAA 26th Aerospace Sciences Meeting, January 1988.